Springer

KSME

Journal of Mechanical Science and Technology 31 (9) (2017) 4363~4369
www.springerlink.com/content/1738-494x(Print)/1976-3824(Online)
DOI 10.1007/s12206-017-0835-4

Highly efficient in-line wet cyclone air sampler for airborne virus detection †

Giwoon Sung[1,*], Chisung Ahn[2], Atul Kulkarni[1], Weon Gyu Shin[3] and Taesung Kim[1,4,*]

[1]*School of Mechanical Engineering, Sungkyunkwan University, 300 Chunchun-dong, Jangan-gu, Suwon 440-746, Korea*
[2]*Department of Nuclear, Plasma, and Radiological Engineering, University of Illinois at Urbana-Champaign, Urbana, IL 61801, USA*
[3]*Department of Mechanical Engineering, Chungnam National University, Daejeon 305-764, Korea*
[4]*SKKU Advanced Institute of Nanotechnology (SAINT), Sungkyunkwan University, 300 Chunchun-dong, Jangan-gu, Suwon 440-746, Korea*

(Manuscript Received May 18, 2017; Revised May 22, 2017; Accepted May 23, 2017)

Abstract

Early detection of highly pathogenic strains is particularly important from the point of view of controlling and minimizing the spread of the virus. Wherein, the sampling of infectious virus from air is a crucial step for effective pandemic disease diagnosis. However, most of the air samplers required long sampling time and real time virus analysis is not possible. Hence, the present work we report design and development of in-line virus detection system by adopting newly designed wet cyclone air sampler. An in line airborne virus detection system composed of preseparator and wet cyclone type impactor for air sampling, fluidics system, and virus sensing platform. All virus detection processes, such as sampling of air, hydration, delivery, and immunoassay were carried out on a single system without any pre- or post-sample treatment. Prior to virus detection, the collection efficiency @ 1000 L/min is tested with PSL particles and is observed that the air sampler efficiency for 1 μm AD is about 50 %, 1.5 μm AD is 78.3 %. And for the large size PSL the observed collection efficiency is about 100 %. Further, it is observed that, the developed system is capable of efficient collection of airborne viral pathogens such as H1N1 and H3N2.

Keywords: Influenza detection; Airborne virus; Lateral flow immunoassay reader; Bio-aerosol; Wet cyclone

1. Introduction

Bioaerosols, such as bacteria, fungi, viruses, and other biological particles (e.g., pollen) can spread diseases of humans, plants, and animals on the scale of meters to continents, due to potential for long-distance transport in the atmosphere. In particular, there is a need to intensify efforts to collect the airborne viruses efficiently in the wake of H1N1 incidences in South Korea and international level [1-5]. In response to the outbreak, health agencies of nations worldwide are busy organizing policies and systems to improve public health, issue quarantines, and treat and prevent widespread outbreaks of influenza. The Highly pathogenic (HP) avian influenza strains, such as H1N1, are particularly important targets for early detection of influenza virus. In order for proper measures to be possible, continuous monitoring of risk factors and early detection is pivotal. Hence, there is a need for highly efficient air virus sampler.

In general, the bioaerosols samplers were classified into four categories such as impingers, cyclones, impactors, and filters. Impingers and cyclones collect airborne particles into a liquid collection medium, whereas impactors collect particles on to solid/semi-solid mediums and filters trap bioaerosol material on fine fibers or porous membrane surfaces. Impingers operate by channeling air flow including particles through nozzles that exit into a chamber containing liquid [6]. Various impingers type Bioaerosol samplers are in use [7-10]. In the cyclone type samplers the aerosols were forced by the shape of the collection chamber into a spiral, swirling flow. Within this airflow, particles experience a centrifugal force proportional to their diameter, density, and speed. This centrifugal force carries particles with sufficient inertia towards the cyclone wall where they are separated from the air flow into a liquid [11, 12]. Many cyclone type bioaerosol samplers were utilized in practice [7, 9, 13-15]. Like the cyclone, the impactor uses the inertia of the particle to facilitate collection [16-20]. However it is not suitable for extensive collection in the outdoors since these bio-aerosol samplers are all designed with low flow rates of 1.5 to 300 L/min. In addition, the above bio-samplers which require a long sampling time are not easy for real-time sampling and detection.

In this paper, we designed and developed an in-line detection system of a 1000 L/min wet cyclone air sampler system which accumulates the floating particles/virus by mixing it with the water for detection with the help of biosensors. The

*Corresponding author. Tel.: +82 31 299 7466, Fax.: +82 31 299 47541
E-mail address: tkim@skku.edu
† Recommended by Associate Editor Dong Geun Lee

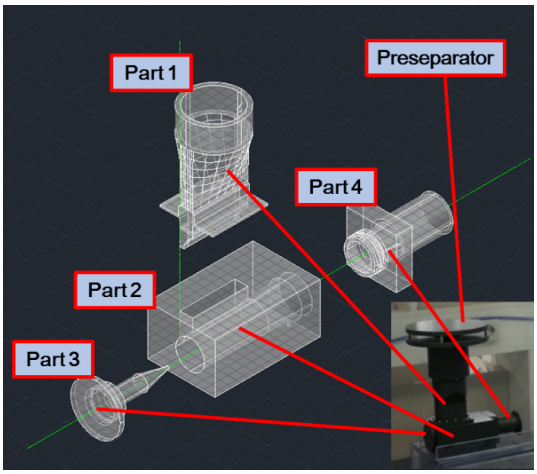

Fig. 1. Image of the proposed the wet cyclone air sampler.

wet cyclone design was evaluated by CFD for particle flow and collection efficiency. Further, the fabricated wet cyclone system was used for the detection of H1N1 virus to show its applicability.

2. Wet cyclone air sampler design

The developed virus detection system consists of three major components: The wet cyclone air sampler, fluidics system, and biosensor strip reader system.

The air sampler is organized into the preseparator [21] and the wet cyclone assembly. The wet cyclone assembly consists of inlet (part 1) to connect to the main body (part 2) in tangential, part 3 is vortex finder to generate vortex flow and part 4 is skimmer as described in the Fig. 1.

It is known that, wet cyclone are generally used to collect and concentrate Bioaerosols in a liquid phase, which is typically water. A cyclone air sampler was designed based on the Stokes number, Stk, and Reynolds number, Re, to collect and concentrate airborne particle in a liquid [23-25]. Stk and Re are defined as [24]:

$$\mathrm{Stk} = \frac{C_c \rho_p d_p^2}{18 \mu W}, \tag{1}$$

$$\mathrm{Re} = \frac{\rho_a U W}{\mu}, \tag{2}$$

where C_c is slip correction factor, ρ_p is density of particle, d_p is aerodynamic particle diameter, U is speed of air in the inlet slot, μ is air viscosity, ρ_a is air density, W is slot width. Differently sized cyclones should equally well collect particles if cyclones are designed and operated with equal values of *Stk* and *Re*.

The dimensions and shape of inlet of wet cyclone is based on the preseparator and the inlet of main body of the wet cyclone. In the present design the diameter of inlet is 58.7 mm and the bottom rectangle of inlet has dimensions of 5.87 mm*58.7 mm (Width*Length). The cyclone main body inlet width is obtained from the Eq. (1), which determines the bioaerosol flow in to the main body. The vortex finder has suitable dimensions to match the main body inlet length. The role of vortex finder is to generate vortex flow of collected bioaerosols. The important aspect here is the vortex finder length should be higher than the main body inlet length and is 70 mm. The role of skimmer is to prevent the water to enter in to the main body and has dimensions 30.4 mm. The fabricated wet cyclone is shown in the Fig. 1 inset.

2.1 CFD analysis of designed wet cyclone.

To evaluate the flow field and particle trajectories in the wet cyclone air sampler, Commercial fluid dynamics (CFD) code FLUENT 17.1 (ANSYS Inc.) solver was used. The time-averaged Navier-stokes equations describe the motion of the turbulent airflow which is treated as 3-D steady incompressible and isothermal in the exposure chamber. Near the inlet the calculated Reynolds number is above 17000, hence the turbulent flow was solved using the realizable k-ε model and the SIMPLE algorithm is applied to compute the pressure corrections during iteration procedure. The convection terms are discretized using the upwind scheme which is the second order in space. The concept of residuals was used in order to ascertain that the iteration process had converged less than 10^{-5} to a stable solution. In addition, the Lagrangian method is simulated with Discrete phase model (DPM) for the particle trajectory. Polystyrene latex (PSL) particles (100 numbers) were spray injected from the inlet at three locations (shown as 1, 2 and 3 in Fig. 2).

ICEM CFD 17.1 (ANSYS Inc.) was used to make about 1 million tetrahedral meshes. The gas flow through the 1000 L/min wet cyclone separator is turbulent in the all parts (particularly 17700 Reynolds number at the rectangle inlet), even though the Reynolds number varies considerably. Based on the Boussinesq hypothesis, the Reynolds-averaged Navier-Stokes equations were solved to predict the continuous phase. Ignoring the mass forces, the equations are described as follows.

Continuous conservation equation:

$$\frac{\partial \rho}{\partial t} + \frac{\partial}{\partial x_i}\left(\rho u_i\right) = 0 . \tag{3}$$

Momentum conservation equation:

$$\frac{\partial}{\partial t}\left(\rho u_i\right) + \frac{\partial}{\partial x_j}\left(\rho u_i u_j\right) = -\frac{\partial p}{\partial x_i} + \frac{\partial \tau_{ij}}{\partial x_j} . \tag{4}$$

Energy conservation equation:

$$\frac{\partial}{\partial t}\left[\rho\left(e + \frac{u_i u_j}{2}\right)\right] + \frac{\partial}{\partial x_j}\left\{u_j\left[\rho\left(e + \frac{u_i u_j}{2}\right) + p\right]\right\} = -\frac{\partial}{\partial x_i}\left(k\frac{\partial T}{\partial x_i} + u_j \tau_{ij}\right) . \tag{5}$$

State equation:

$$\frac{p}{\rho} = RT \tag{6}$$

where

$$\tau_{ij} = (\mu + \mu_T)\left(\frac{\partial u_i}{\partial x_j} + \frac{\partial u_j}{\partial x_i}\right) - \frac{2}{3}\delta_{ij}(\mu + \mu_T)\frac{\partial u_k}{\partial x_k}. \tag{7}$$

The two-equation turbulence model, realizable k-ε model, was used to simulate the turbulence transport effects. The transport equations for k and ε in the realizable k-ε model are as follows:

$$\frac{\partial(\rho k)}{\partial t} + \frac{\partial(\rho k u_i)}{\partial x_i} = \frac{\partial}{\partial x_i}\left[\left(\mu + \frac{\mu_T}{\sigma_k}\right)\frac{\partial k}{\partial x_i}\right] + G_k + G_b - \rho\varepsilon - Y_M + S_k \tag{8}$$

$$\frac{\partial(\rho \varepsilon)}{\partial t} + \frac{\partial(\rho \varepsilon u_i)}{\partial x_i} = \frac{\partial}{\partial x_i}\left[\left(\mu + \frac{\mu_T}{\sigma_\varepsilon}\right)\frac{\partial \varepsilon}{\partial x_i}\right] + \rho C_1 S\varepsilon - \rho C_2 \frac{\varepsilon^2}{k + \sqrt{\nu\varepsilon}}. \tag{9}$$

The model constants have been determined from the experiments and are given as follows:

$$C_{1\varepsilon} = 1.44,\ C_{2\varepsilon} = 1.9,\ C_\mu = 0.09,$$
$$\sigma_k = 1.0,\ \sigma_\varepsilon = 1.2. \tag{10}$$

3. PSL particles collection efficiency

Fig. 2 shows the particles trajectory results in the wet cyclone. Micro-sized water droplets are injected into the system which creates a water film on the surface of the wet cyclone allowing for a condensed solution sample. At each of the positions, insertion of 100 particles of 1 μm size in Aerodynamic diameter (AD) resulted in a collection efficiency of 17 %, 80 % and 42 %, respectively as shown in Fig. 2(a). Particles injected in the middle were collected on the wall with high efficiency, however particles sprayed on the side showed relatively low efficiency. Particularly, particles injected at a position adjacent to the vortex finder did not have enough acceleration to achieve a particle velocity that would hit the wall. Fig. 2(b) shows that 35 %, 100 % and 100 % of 1.5 μm AD particles were collected at each location. As the particle size increased, the collection efficiency increased because the inertial force and centrifugal force acting on the particles increased. Total efficiency of 1 μm AD is about 46.3 %, 1.5 μm AD is 78.3 μm. Fig. 2(c) shows that all the particles collide with the cyclone wall even if the particles of 2 μm AD are sprayed from any position. Since the losses by bouncing of the particles at the cyclone inner wall is not considered, the collection efficiency for the large sizes (≥ 2 μm) is about 100 %.

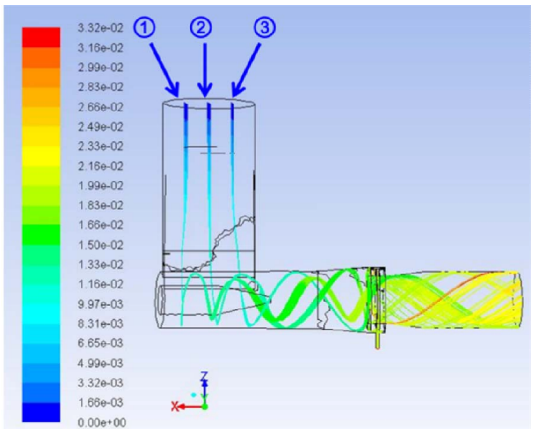

(a)

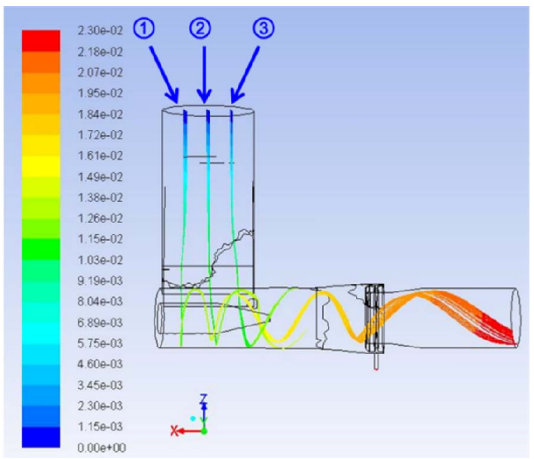

(b)

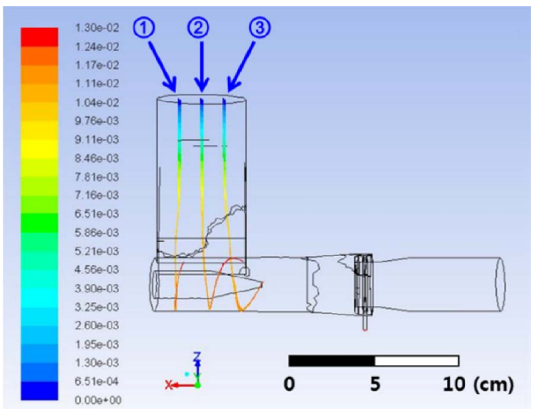

(c)

Fig. 2. Particles trajectory in the wet cyclone simulated by DPM at a sampling flow rate of 1000 L/min; sprayed monodisperse particle size: (a) 1 μm; (b) 1.5 μm; (c) 2 μm.

Fig. 3 shows the experimental set-up for the measurement of collection efficiency of the cyclone air sampler. The set-up consists of a particle generation system and the efficiency measurement system. The PSL with micro-size in a range 0.45 to 3 μm Aerodynamic diameter (AD) with the density of

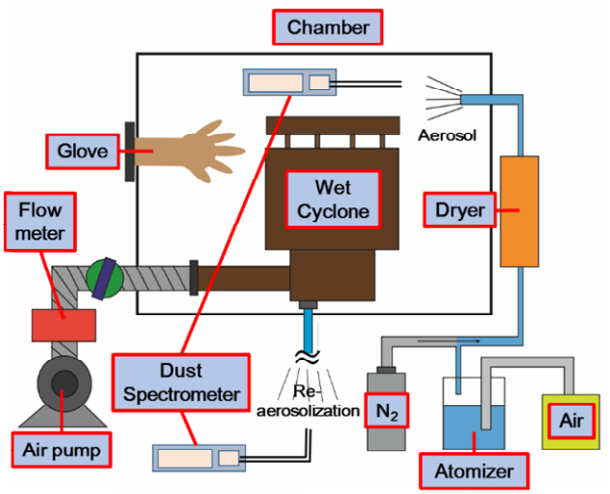

Fig. 3. Experimental set-up; schematic diagram of an experimental set-up for the measurement of the collection efficiency of the wet cyclone air sampler.

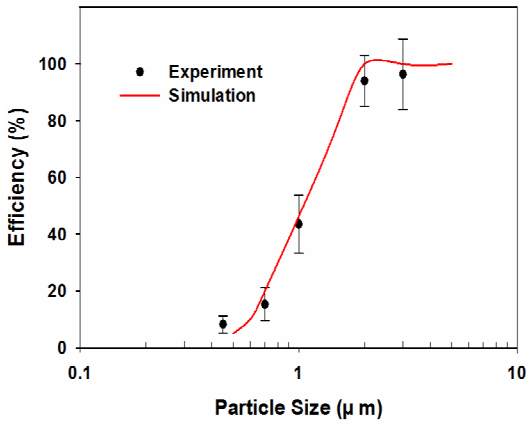

Fig. 4. Collection efficiency results of the wet cyclone air sampler; experimental and simulation results for aerosol-to-hydrosol collection efficiency.

1050 kg/m^3 was generated by atomizer in the chamber with volume of 1 m^3 and the particles were transported by an air pump (DJM 2RB 510-7AH36) with the flow rate of 1000 L/min. The nozzles were installed at the inlet of the cyclone to spray water at a flow rate of 5 mL/min. In order to obtain the efficiency of the number concentrations in the air inlet and concentrate part of the cyclone air sampler were measured using a dust spectrometer (Grimm, Model 1.109). In addition, to measure the number concentration of the hydrosol using the dust spectrometer, the particles collected in water were re-aerosolized. Commonly used performance parameters to calculate the collection efficiency of a cyclone or impactor are aerosol-to-aerosol collection efficiency. However, the aerosol-to-aerosol collection efficiency does not distinguish between particle losses on internal surfaces and particles transported from the cyclone in the hydrosol state. The aerosol-to-hydrosol collection efficiency of a wet cyclone is defined as the ratio of the rate at which particles of a specified size leave the cyclone in the hydrosol state to the rate at which they enter in the aerosol state, and can be expressed as:

$$\eta_{AH} = \frac{c_{l,e} Q_l}{c_{a,\infty} Q_a} \tag{11}$$

where $c_{l,e}$ is concentration of particles of the specified size in the hydrosol state at the liquid exit port, Q_l = volumetric flow rate of liquid at the exit port, Q_a = volumetric flow rate of air at the cyclone entrance port, i.e., the aerosol sampling flow rate [23]. For wet cyclone, the aerosol-to-hydrosol collection efficiency more suitably describes the performance than does the aerosol-to-aerosol collection efficiency because particle losses in the cyclone are deducted.

Particle collection efficiency results are shown in Fig. 4 for tests conducted with the cyclone air sampler to characterize the aerosol-to-hydrosol collection efficiency, η_{AH}, as functions of particle size. Solid monodisperse PSL was used as the test aerosol for sizes < 3 μm AD. As shown in Fig. 4, the wet cyclone air sampler has a cutpoint of about 1.0 μm AD and high value (≥ 95 %) of η_{AH} for particles with sizes of more than 2 μm AD. The experimental collection efficiency results are slightly lower compared to the simulation results, since no water film is generated in some parts of the cyclone inner wall. It is well known that, the size range of bioaerosols varies from submicron-size (viral particles, fungal spores and pollen grains) up to 1 mm in diameter. Hence, the wet cyclone air sampler developed in this study is expected to capture most types of bioaerosols efficiently due to the characteristics of the wet cyclone that collects based on inertia and centrifugal force.

4. Virus detection system design

The fluidics control system was designed to maintain the appropriate flow of water and solution needed for collection in the air sampler and for dispensing solution samples to the biosensor for detection [26-28]. Fig. 5(a) depicts the overall virus detection system including designed in-line wet cyclone. Fig. 5(b) shows the actual photo of the system including the air sampler (b-1), the biosensor strip reader (b-2) and fluidics control system (b-3). For the biosensor strip reader system, we developed a system based on the lateral flow immunoassay strip (also called immunochromatographic assay or test strip) used in rapid analytical diagnosis techniques [22]. The fluidics control system was implemented using a micro diaphragm liquid pump (NF11 KPDC) and 3-way solenoid valves (LFR Series). From the fluidics control system schematics in the Fig. 5(a), pump 3 was set to have a flow less than 5 ml/min and the others were set at an output of 10 ml/min. The water solution circulates the entire system continuously allowing for concentration of airborne particles with the pump 3. The system is set to dispense 100 μl of the collected solution onto the virus sensor by the 3-way solenoid valves connected to pump 2.

Two types of virus vaccine solutions were used for the ex-

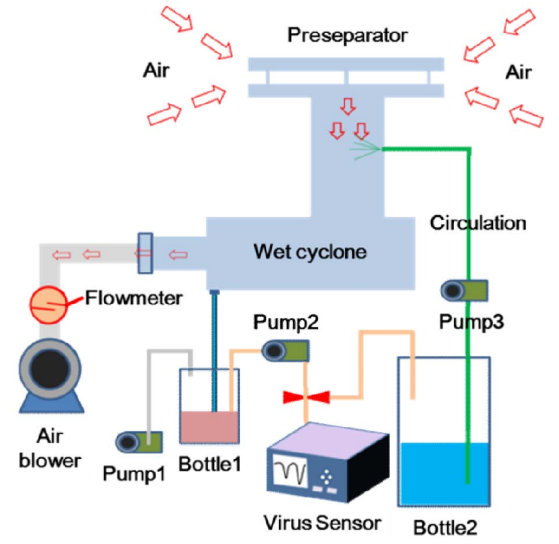

(a)

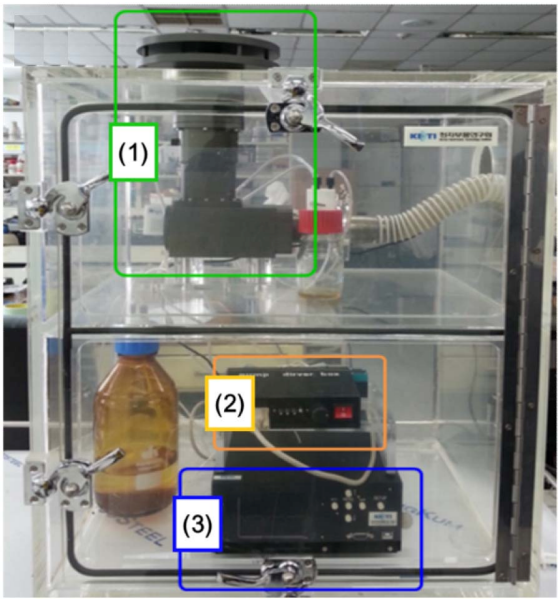

(b)

Fig. 5. Setup for virus detection: (a) Schematic diagram of fluidics system and image of prototypes of flow control and pump control board; (b) Image of the proposed airborne virus detection system constructed; (b-1) the cyclone air sampler; (b-2) the biosensor strip reader; (b-3) micro fluidics control system.

periment: the human infectious influenza type H1N1 and H3N2 of Novartis Vaccines and Diagnostics S.r.l. The vaccine solution for each of the types of virus was diluted using the appropriate buffer solution and dispersed into the environment to be collected with the air sampler during the experiment. Fig. 6 shows the results for H1N1 virus and H3N2 virus. For the influenza virus, it was observed that since a single strip is used to target the two different antigens of H1N1 and H3N2, the intensity of the line that forms on the strip for the H3N2 virus B type has an overall lower intensity than the line for the

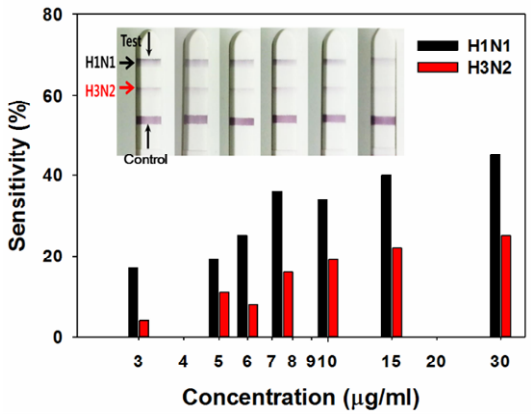

Fig. 6. Results of experiments to detect human infectious influenza (H1N1, H3N2 virus) in air; Images of influenza (H1N1, H3N2) strip sensor according to dilution ratio and comparison of concentration to normalized current level signal intensity (ΔI/I0) for the two different types of influenza.

H1N1 target.

Detection of virus was realized using influenza virus Lateral flow immunoassay (LFIA) strips [29, 30]. Collected solution samples are dispensed onto the strip which forms a conjugate with the antigen nanoparticles and is subsequently captured at the detection line. A strip reader system to quantitatively measure the intensity of the detection line was developed in this paper. The strip reader system consists of a mechanical stage to dispense the sample solution onto the strip and transport the strip within the system and also an optical reading stage. We developed the method of data acquisition from the LFIA strip biosensor in a previous work [31]. The optical reading stage exposes the strip with light from a laser diode and measures the reflected light from the strip using a photodiode [32-35]. The intensity of the measured light signal changes according to the density of nanoparticles on the surface of membrane. The intensity of the signal, which is measured as a current level, is calculated as a sensitivity value. The sensitivity values are normalized according to the base line level, I_0, and calculated as $\Delta I/I_0$ from real-time scanning results [32-35].

5. Conclusions

In this paper, we have successfully presented an airborne virus detection system for monitoring pathogens and demonstrated the operation with bioaerosols. We have successfully prototyped the system by developing an in-line wet cyclone air sampler system, fluidics system. The experimental evaluations shows the quantitative measurement of virus concentration in the air, thus verifying the operation of in-line wet cyclone system. We believe that the developed system can be utilized in various applications of security such as early detection of biological hazards or dangerous airborne virus in public areas.

Acknowledgment

This work was supported by a National Research Foundation of Korea (NRF) grant funded by the Korean government (NRF-2016M3A7B4909649).

References

[1] J. Lum et al., Rapid detection of avian influenza H5N1 virus using impedance measurement of immuno-reaction coupled with RBC amplification, *Biosensors & Bioelectronics*, 38 (1) (2012) 67-73.

[2] Y. T. Kim et al., Integrated microdevice of reverse transcription-polymerase chain reaction with colorimetric immunochromatographic detection for rapid gene expression analysis of influenza A H1N1 virus, *Biosensors & Bioelectronics*, 33 (1) (2012) 88-94.

[3] F. Stripeli et al., Performance of rapid influenza testing in hospitalized children, *European Journal of Clinical Microbiology & Infectious Diseases*, 29 (6) (2010) 683-688.

[4] S. Marche and T. van den Berg, Evaluation of rapid antigen detection kits for the diagnosis of highly pathogenic avian influenza H5N1 infection, *Avian Diseases*, 54 (s1) (2010) 650-654.

[5] M. E. Alexander et al., Emergence of drug resistance: implications for antiviral control of pandemic influenza, *Proceedings of the Royal Society B: Biological Sciences*, 274 (2007) 1675-1684.

[6] D. Sykes, *The development of a bioaerosol sampler for the detection of enzymes in industry*, University of Teesside, UK (2005).

[7] A. Hoisington et al., The impact of sampler selection on characterizing the indoor microbiome, *Building and Environment*, 80 (2014) 274-282.

[8] L. Wen-Hai and L. Chih-Shan, Influence of storage on the fungal concentration determination of impinger and filter samples, *Am Indust. Hyg. Assoc. J.*, 64 (1) (2003) 102-107.

[9] V. Langer et al., Rapid quantification of bioaerosols containing L. pneumophila by Coriolis μ air sampler and chemiluminescence antibody microarrays, *Journal of Aerosol Science*, 48 (2012) 46-55.

[10] D. Saini et al., Sampling port for real-time analysis of bioaerosol in whole body exposure system for animal aerosol model development, *Journal of Pharmacological and Toxicological Methods*, 63 (2) (2011) 143-149.

[11] W. Peng et al., Reverse-flow centrifugal separators in parallel: performance and flow pattern, *Am Inst. Chem. Engrs J.*, 53 (3) (2007) 589-597.

[12] T. Mothila and K. Pitchandi, Influence of inlet velocity of air and solid particle feed rate on holdup mass and heat transfer characteristics in cyclone heat exchanger, *Journal of Mechanical Science and Technology*, 29 (10) (2015) 4509-4518.

[13] R. S. Dungan, Use of a culture-independent approach to characterize aerosolized bacteria near an open-freestall dairy operation, *Environment International*, 41 (2012) 8-14.

[14] J. Macher et al., Field evaluation of a personal, bioaerosol cyclone sampler, *Journal of Occupational and Environmental Hygiene*, 5 (11) (2008) 724-734.

[15] A. D. Tolchinsky et al., Development of a personal bioaerosol sampler based on a conical cyclone with recirculating liquid film, *Occupational and Environmental Hygiene*, 7 (3) (2010) 156-162.

[16] R. Persoons et al., Critical working tasks and determinants of exposure to bioaerosols and MVOC at composting facilities, *International Journal of Hygiene and Environmental Health*, 213 (5) (2010) 338-347.

[17] B. K. Lavine et al., Prediction of mold contamination from microbial volatile organic compound profiles using head space gas chromatography/mass spectrometry, *Microchemical Journal*, 103 (2012) 37-41.

[18] C. W. Park et al., Effects of condensational growth on culturability of airborne bacteria: implications for sampling and control of bioaerosols, *Journal of Aerosol Science*, 42 (2011) 213-223.

[19] R. C. Spicer et al., Differences in detection frequency as a bioaerosol data criterion for evaluating suspect fungal contamination, *Building and Environment*, 45 (5) (2010) 1304-1311.

[20] S. Zhen et al., A comparison of the efficiencies of a portable BioStage impactor and a Reuter centrifugal sampler (RCS) High Flow for measuring airborne bacteria and fungi concentrations, *Journal of Aerosol Science*, 40 (6) (2009) 503-513.

[21] M. Son et al., Development of a novel aerosol impactor utilizing inward flow from a ring-shaped nozzle, *Journal of Aerosol Science*, 85 (2015) 1-9.

[22] B. Ngom et al., Development and application of lateral flow test strip technology for detection of infectious agents and chemical contaminants: a review, *Analytical and Bioanalytical Chemistry*, 397 (3) (2010) 1113-1135.

[23] A. R. McFarland et al., Wetted wall cyclones for bioaerosol sampling, *Aerosol Science and Technology*, 44 (4) (2010) 241-252.

[24] W. C. Hinds, *Aerosol technology: Properties, behavior, and measurement of airborne particles*, Wiley, New York and Chichester (1999) 190-195.

[25] S. S. Hu and A. R. McFarland, Numerical performance simulation of a wetted wall bioaerosol sampling cyclone, *Aerosol Science and Technology*, 41 (2) (2007) 160-168.

[26] P. Skladal et al., Electrochemical immunosensor coupled to cyclone air sampler for detection of escherichia coli DH5 alpha in bioaerosols, *Electroanalysis*, 24 (3) (2012) 539-546.

[27] J. A. Hubbard et al., Liquid consumption of wetted wall bioaerosol sampling cyclones: Characterization and control, *Aerosol Science and Technology*, 45 (2) (2011) 172-182.

[28] J. M. Blatny et al., Tracking airborne Legionella and Legionella pneumophila at a biological treatment plant, *Environmental Science & Technology*, 42 (19) (2008) 7360-7367.

[29] S. Bamrungsap et al., Rapid and sensitive lateral flow im-

munoassay for influenza antigen using fluorescently-doped silica nanoparticles, *Microchimica Acta*, 181 (1) (2014) 223-230.

[30] N. Nagatani et al., Detection of influenza virus using a lateral flow immunoassay for amplified DNA by a microfluidic RT-PCR chip, *Analyst*, 137 (2012) 3422-3426.

[31] K. J. Jang et al., Optical reading system for quantitative analysis of lateral flow assay (LFA) based immunological diagnostic kits, *Proceedings of the The Korean BioChip Society* (2014) PIII-2-12.

[32] F. Zhang et al., Lanthanide-labeled immunochromatographic strips for the rapid detection of Pantoea stewartii subsp stewartii, *Biosensors & Bioelectronics*, 51 (15) (2014) 29-35.

[33] W. Y. Zhang et al., Direct, analysis of trichloropyridinol in human saliva using an Au nanoparticles-based immunochromatographic test strip for biomonitoring of exposure to chlorpyrifos, *Talanta*, 114 (30) (2013) 261-267.

[34] W. Xu et al., Ru(phen)(3)(2+) doped silica nanoparticle based immunochromatographic strip for rapid quantitative detection of beta-agonist residues in swine urine, *Talanta*, 114 (30) (2013) 160-166.

[35] W. Wu et al., A lateral flow biosensor for the detection of human pluripotent stem cells, *Analytical Biochemistry*, 436 (2) (2013) 160-164.

Giwoon Sung received his Bachelor of Science degree in Mechanical Engineering from Sungkyunkwan University of Technology, Korea in 2011. Currently, he is a candidate in the combined master's and doctorate program in the School of Mechanical Engineering at Sungkyunkwan University. His research is focused on the numerical analysis of particles suspended in fluid.

Taesung Kim received his Bachelor of Science degree in Mechanical Engineering from Seoul National University of Technology, Korea in 1994. He received his Master of Science and Doctor of Philosophy degrees in Mechanical Engineering from the University of Minnesota, Minneapolis, MN, USA in 1998 and 2002, respectively. Dr. Kim currently works as a Professor in the School of Mechanical Engineering and as an Adjunct Professor at the SKKU Advanced Institute of Nano Technology at Sungkyunkwan University in Suwon, Korea. His research interests include nanoparticle synthesis, development of applications related to bio aerosols, Chemical Mechanical Polishing and thin film synthesis.